4988 *Inorg. Chem.* **2009,** *48,* 4988–4996
DOI:10.1021/ic900146y

Inorganic Chemistry
Article

Temperature Dependence of Single-Crystal Elastic Constants of Flux-Grown α-$GaPO_4$

P. Armand,*,† M. Beaurain,† B. Rufflé,‡ B. Menaert,§ and P. Papet†

†*Institut Charles Gerhardt Montpellier, UMR5253 CNRS-UM2-ENSCM-UM1, PMOF, UMII, CC1504, Place E. Bataillon, 34095 Montpellier Cedex 5, France,* ‡*Laboratoire des Colloïdes, Verres et Nanomatériaux, UMR5587, UMII CC069, 34095 Montpellier Cedex 5, France, and* §*Département Matière Condensée, Matériaux et Fonctions, Institut Néel/CNRS-UJF, BP 166, 38042 Grenoble Cedex 09, France*

Received January 22, 2009

The lattice parameter change with respect to temperature (T) has been measured using high-temperature powder X-ray diffraction techniques for high-temperature flux-grown $GaPO_4$ single crystals with the α-quartz structure. The lattice and the volume linear thermal expansion coefficients in the temperature range 303−1173 K were computed from the X-ray data. The percentage linear thermal expansions along the *a* and *c* axes at 1173 K are 1.5 and 0.51, respectively. The temperature dependence of the mass density ρ of flux-grown $GaPO_4$ single crystals was evaluated using the volume thermal expansion coefficient $\alpha_V(T) = 3.291 \times 10^{-5} - 2.786 \times 10^{-8}[T] + 4.598 \times 10^{-11}[T]^2$. Single-crystal high-resolution Brillouin spectroscopy measurements have been carried out at ambient pressure from 303 to 1123 K to determine the elastic constants C_{IJ} of high-temperature flux-grown $GaPO_4$ material. The single-crystal elastic moduli were calculated using the sound velocities via the measured Brillouin frequency shifts $\Delta\nu_B$. These are, to our knowledge, the highest temperatures at which single-crystal elastic constants of α-$GaPO_4$ have been measured. Most of the room-temperature elastic constant values measured on flux-grown $GaPO_4$ material are higher than the ones found for hydrothermally grown $GaPO_4$ single crystals. The fourth-order temperature coefficients of both the Brillouin frequency shifts $T_{\nu B}^{(n)}$ and the single-crystal elastic moduli $T_{C_{IJ}}{}^{(n)}$ were obtained. The first-order temperature coefficients of the C_{IJ} are in excellent agreement with previous reports on low-temperature hydrothermally grown α-$GaPO_4$ single crystals, while small discrepancies in the higher-order temperature coefficients are observed. This is explained in terms of the OH content in the $GaPO_4$ network, which is an important parameter in the crystal thermal behavior.

Introduction

Knowledge of single-crystal elastic moduli at high temperatures is important in the development of high-temperature materials. The most complete and accurate set of elasticity data comes from measurements of acoustic velocities in single-crystal samples. Sound velocities in specified crystallographic directions, and hence elastic constants, can be easily measured using Brillouin scattering on samples as small as 100 μm.[1] This experimental technique provides a powerful method of determining room- and high-temperature single-crystal elastic properties for materials which are not produced in sufficiently large sizes for conventional ultrasonic techniques. The single-crystal elastic modulus is calculated using the measured velocity of sound, deduced from the Brillouin frequency shift, and the mass density. For high-temperature elastic constant determination, an accurate knowledge of the temperature dependence of the density of the sample is required.

Gallium orthophosphate $GaPO_4$ material with the low-temperature quartz structure (α-quartz) belongs to the class of compounds with the general formula $M^{3+}X^{5+}O_4$. Interest in single crystals of $GaPO_4$ comes from the fact that this piezoelectric material possesses nearly all of the advantages of quartz, but it has a higher electromechanical coupling for the same AT cut and has thermally stable physical properties up to 1203 K.[2,3] Indeed, at atmospheric pressure, there is no α↔β quartz transition for $GaPO_4$, which exhibits only a transition into a nonpiezoelectric cristobalite-like phase toward 1223 K.[4,5] Furthermore, α-$GaPO_4$

*To whom correspondence should be addressed. Phone: (+33) 4 67 14 33 19. Fax: (+33) 4 67 14 42 90. E-mail: pascale.armand@.univ-montp2.fr.

(1) Weidner, D. J.; Carleton, H. R. *J. Geophys. Res.* **1977**, *82*, 1334.
(2) Cambon, O.; Goiffon, A.; Philippot, E. *J. Solid State Chem.* **1989**, *78*, 187.
(3) Philippot, E.; Ibanez, A.; Goiffon, A.; Capelle, B.; Zarka, A.; Schwartzel, J.; Détaint, J. In *Proceedings of the 36th European Frequency and Time Forum*; ENSMM: Besançon, France, 1992; p 383.
(4) Beaurain, M.; Armand, P.; Papet, P. *J. Cryst. Growth* **2006**, *294*, 396.
(5) Jacobs, K.; Hofmann, P.; Klimm, D.; Reichow, J.; Scneider, M. *J. Solid State Chem.* **2000**, *149*, 180.

 Published on Web 4/27/2009

shows a very slow propagation of surface acoustic waves (SAW).[6] These characteristics allow $GaPO_4$ to be used in the field of high-temperature pressure sensors as well as SAW applications.

The synthetic α-quartz $GaPO_4$ single crystals were commonly grown in acidic media using low-temperature hydrothermal methods below 523 K.[7,8] In this temperature range and at low pressure ($P < 2$ MPa), the solubility of $GaPO_4$ shows a negative temperature coefficient (retrograde solubility) in all applied solvents.[8,9] The hydrothermally grown $GaPO_4$ single crystals are transparent, well-faceted, and can be obtained in the centimeter size range.[10] However, these crystals contain hydroxyl groups (OH), most often in appreciable content, which affects their piezoelectric properties and may limit their use at high temperatures.[8,11]

The high-temperature flux-growth method consists of using mineral fluxes as solvents for growing α-$GaPO_4$ single crystals at temperatures below their allotropic transformation.[12−14] The interesting effect of both the anhydrous solvent and the high temperature is a prevention of hydroxyl group incorporation during growth experiments. From room-temperature infrared measurements in the transmission mode, the virgin flux-grown α-$GaPO_4$ crystals have been found, as expected, free from OH impurities. Another important result concerns the thermal behavior of these as-grown materials. A totally reversible α-quartz ↔ β-cristobalite phase transition from the first thermal cycle was registered using differential thermal analysis.[4]

A first room-temperature determination of four out of six single-crystal elastic constants was previously undertaken using the ultrasonic method on millimeter plates.[14] These preliminary results were very encouraging and had to be completed through the determination of the other elastic constants. Moreover, for high-temperature applications, the temperature dependence of the elastic properties has to be determined. For this purpose, the knowledge of the bulk thermal expansion coefficient is essential for the calculation of elastic constants as a function of the temperature. Thus, reliable values are needed, and the most common method to determine thermal expansion coefficients is the measurement of lattice parameters at various temperatures using powder or single-crystal X-ray diffraction (XRD) methods. This paper reports on a first thermal expansion coefficient determination of the high-temperature flux-grown α-$GaPO_4$ single-crystals as well as the temperature dependence of several elastic constants C_{IJ} (at constant electric field). The obtained results are discussed and compared with previous reports on low-temperature hydrothermally grown α-$GaPO_4$ single crystals.

Experimental Procedure

Flux-Grown Samples. Optical-quality single crystals of α-$GaPO_4$ at millimeter size were flux-grown from a $Li_2O-3MoO_3$ solvent in unseeded experiments over the temperature range 873−1223 K.[4,12] Both the space group and the unit cell parameters were verified using room-temperature singe-crystal X-ray diffraction. All of the virgin, high-temperature flux-grown crystals are colorless, transparent, and show the low-quartz (or α-quartz) equivalent berlinite structure.[4,12,13] No trace of any other gallium phosphate phase was detected. The as-grown crystals did not exhibit well-formed faces, and thus Laue patterns were necessary to identify crystallographic plans normal to the Cartesian X, Y, or Z axes. An as-grown $GaPO_4$ sample was polished as a cube with a 2 mm side length showing X (100), Y (010), and Z (001) faces. The accuracies of size and orientations were ±1 μm and ±0.6°, respectively.

Instrumental Setup. The temperature dependence of XRD at temperatures from 303 to 1173 K was determined using a Philips PW1050 X-ray diffractometer equipped with an Anton Paar HTK16 attachment and with a curved graphite monochromator. The well ground sample was mounted on a platinum strip which served as a sample holder and as a heater. The temperature was monitored by a Pt−Pt/Rd thermocouple and stabilized with the aid of a temperature controller to within ±0.5 K. The sample was heated to the desired temperature at a rate of 120 °C/min and held for 30 min. All measurements were carried out in a vacuum of about 10^{-5} Torr. Integrated intensities were scanned using the Cu Kα radiation under normal atmospheric conditions in the 2θ range 18−118° with a step interval of 0.04° and a step time of 7.0 s. The unit cell parameters and lattice volume were determined from the observed d spacings by Le Bail refinements using the $GaPO_4$ low-quartz structure model with the FULLPROF software package.

A high-resolution Brillouin spectrometer (HRBS)[15] was used to determine the elastic constants of our flux-grown α-$GaPO_4$ single crystals. The sample was placed on a goniometer and received an incident wavelength λ equal to 514.5 nm provided by a 200 mW, linearly polarized, single-mode line of a Spectra Physics 2060 BeamLock argon laser. The laser light was focused on the sample with a beam diameter of about 15 μm. The backscattered light was analyzed by a HRBS which contained two Fabry−Perot (FP) interferometers in series. The first FP is a four-pass planar FP of 1.5 mm spacing which is maintained at a fixed spacing. It is dynamically adjusted to one of the Brillouin lines with the help of an electro-optically modulated signal at the Brillouin frequency. This FP acts as a band-pass filter of about 1 GHz, eliminating other spectral components and reducing considerably the elastic signal strength. The frequency analysis is done by the second FP, which is a confocal one of 25 mm spacing. Its instrumental full width is about 60 MHz, and its spectral range is 3 GHz. Each Brillouin spectrum is the result of 50−1000 summed scans depending on the scattering intensity of the modes observed. The high-resolution setup of the spectrometer enables us to determine the Brillouin peak frequency very accurately and, thus, to detect very small sound velocity or elastic constant variations. The spectrometer is also equipped with a microscope, which permits backscattering experiments on small-sized samples with an improved spatial, lateral, and depth resolution. For high-temperature measurements, a TS1500 Linkam microscope heating stage was used. The temperature of the samples was regulated with a stability of ±1 K.

Velocity. Atoms inside a solid move in thermal equilibrium with very small amplitudes bringing fluctuations in the dielectric constant, which in turn translate into fluctuations in the

(6) Palmier, D. Ph.D. thesis, UMII, Montpellier, France, 1996.
(7) Philippot, E.; Ibanez, A.; Goiffon, A.; Cochez, M.; Zarka, A.; Capelle, B.; Schwartzel, J.; Détaint, J. *J. Cryst. Growth* **1993**, *130*, 195.
(8) Yot, P.; Cambon, O.; Balitsky, D.; Goiffon, A.; Philippot, E.; Capelle, B.; Détaint, J. *J. Cryst. Growth* **2001**, *224*, 294.
(9) Hirano, S.; Kim, P. C. *J. Mater. Sci.* **1991**, *26*, 2805.
(10) Philippot, E.; Goiffon, A.; Ibanez, A. *J. Cryst. Growth* **1996**, *160*, 268.
(11) Marinho, E.; Palmier, D; Goiffon, A.; Philippot, E. *J. Mater. Sci.* **1998**, *33*, 2825.
(12) Beaurain, M.; Armand, P.; Papet, P. *J. Cryst. Growth* **2005**, *275*, 279.
(13) Shvanskii, E; Armand, P.; Balitsky, D.; Philippot, E.; Papet, P. *Ann. Chim. Sci. Mater.* **2006**, *31*(1), 97.
(14) Beaurain, M.; Armand, P.; Détaint, J.; Balitsky, D.; Papet, P. *J. Phys.: Condens. Matter* **2008**, *20*, 025226.
(15) Vacher, R.; Ayrinhac, S.; Foret, M.; Rufflé, B.; Courtens, E. *Phys. Rev. B* **2006**, *74*, 012203.

refractive index. These fluctuations result in inelastic scattering of the light as it passes through the solid. The Brillouin scattering due to the inelastic interaction of an incident photon with acoustic phonons in a crystal results in a frequency shift $\pm\Delta\nu_B$ of the scattered light relative to the laser frequency, which is related to the velocity of the acoustic phonon v by

$$v = \frac{\Delta\nu_B\lambda}{(n_2^i + n_2^s - 2n_i n_s \cos\theta)^{1/2}} \quad (1)$$

where λ is the wavelength of the incident laser light, n_i and n_s are respectively the refractive indices of the crystal for incident and scattered light directions, and θ is the scattering angle.

In a backscattering geometry, the expression of the sound velocity is thus given by

$$v = \frac{\Delta\nu_B\lambda}{n_i + n_s} \quad (2)$$

$GaPO_4$ crystals with the α-quartz structure are uniaxial crystals with optical birefringence. Due to this birefringence, the Brillouin shift depends on the polarization of the incident and scattered light.

The room temperature values of the ordinary $n_o = 1.6147$ and extraordinary $n_e = 1.6332$ refractive indices at 514.5 nm used in this work were extracted from measurements on hydrothermally grown α-$GaPO_4$ single crystals in the wavelength region from 440 to 1060 nm.[16] Due to the small variation of n_o and n_e with the temperature,[16] their values were considered in the formula as a constant independent of the temperature variation.

Elastic Constants. From the determinations of the sound velocities of the observed acoustic modes of our material, several elastic constants can be deduced with the help of the eigenvalue equation

$$\det[\sum_{j,k=1}^{3} C^*_{ijkl} - \rho v^2\delta_{il}] = 0 \quad (3)$$

with the piezoelectric correction given by

$$C^*_{ijkl} = C^E_{ijkl} + \frac{\sum_{m,n=1}^{3} e_{m,ij}e_{n,kl}Q_mQ_n}{\sum_{m,n=1}^{3} \varepsilon_{mn}Q_mQ_n} \quad (4)$$

δ_{il} is the Kronecker delta and ρ is the mass density of $GaPO_4$. $C_{ijkl}{}^E$, $e_{m,ij}$ and ε_{mn} are components of the elastic, piezoelectric stress, and dielectric permittivity tensors, respectively. The superscript E indicates the condition of constant electric field.

According to the point group 32, α-$GaPO_4$ material has six independent elastic moduli $C_{IJ}{}^E$ (I, J from 0 to 6), C^E_{11}, C^E_{33}, C^E_{44}, C^E_{66}, C^E_{13}, and C^E_{14} ($C^E_{12} = C^E_{11} - 2C^E_{66}$). The average small size of the flux-grown $GaPO_4$ single crystals, 4−6 mm in length, did not allow us to get rotated orientations, which would allow us the measurements of the C_{13} single crystal elastic constant.

(16) Defregger, S.; Engel, G. F.; Krempl, P. W. *Phys. Rev. B* **1991**, *8*, 6733.

Table 1. Scattering Geometries and Expressions of ρv^2 as a Function of the Elastic Constants C_{IJ} at Constant Electric Field for the Oustic Modes (As Defined in Tablustic Modes of the Sample Studied in This Work)

propagation	polarization[a]	mode	expression of ρv^2
X [100]	L	γ_1	$C_{11} + e_{11}^2/\varepsilon_{11}$
Y [010]	T	γ_2	$C_{66} + e_{11}^2/\varepsilon_{11}$
Y [010]	PL	γ_3	$(C_{44} + C_{11})/2 + [(C_{44} - C_{11})^2 + 4C_{14}^2]^{1/2}/2$
Z [001]	L	γ_4	C_{33}
Z [001]	T	γ_5	C_{44}

[a] L = longitudinal, T = transverse, PL = pseudo-longitudinal.

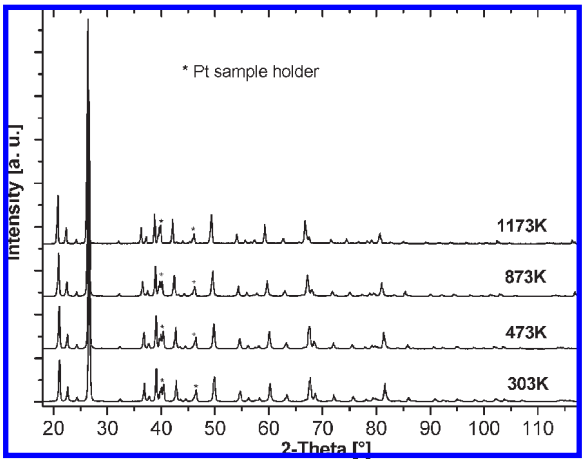

Figure 1. Powder X-ray diffraction patterns of flux-grown α-$GaPO_4$ sample registered at various temperatures.

In Table 1 are gathered the expressions at constant electric field (for simplification, $C_{IJ} = C_{IJ}{}^E$) of the single-crystal elastic moduli $C_{IJ} = \rho v^2$ corresponding to the observed acoustic modes from our sample of X, Y, and Z simple orientations.

The propagation directions to be measured first were those for which the relationship between the elastic constant C_{IJ} and the sound velocity v was the simplest. It was in the form $C_{IJ} = \rho v^2$ for C_{33} and C_{44}, or when the piezoelectric effect had to be taken into account, the relationship was in the form $C_{IJ} = \rho v^2 - e_{11}^2/\varepsilon_{11}$ as for C_{11} and C_{66}. In this work, the value of the piezoelectric effect with the temperature was fixed as $e_{11}^2/\varepsilon_{11} = 0.79 \times 10^9$ N m^{-2}, a room temperature value taken from hydrothermally grown $GaPO_4$ material.[6,17]

Second, we measured the propagation directions for which the sound velocity is no more a function of only one constant but of a combination of several elastic constants, see Table 1. The extraction of the desired constant is done by the differentiation of the other constants for which we have already determined the values.

Results and Discussion

Thermal Expansion. For this work, the high-temperature studies have been restricted up to 1173 K due to the reconstructive phase transformation of the low-quartz-like structure $GaPO_4$ to the high-cristobalite form which arises toward 1223 K.[12,18]

(17) Wallnöfer, W.; Krempl, P.; Asenbaum, A. *Phys. Rev. B* **1994**, *49*, 10075.

(18) Angot, E.; Le Parc, R.; Levelut, C.; Beaurain, M.; Armand, P.; Cambon, O.; Haines, J. *J. Phys.: Condens. Matter* **2006**, *18*, 4315.

Table 2. Density; Refined Unit Cell Parameters *a*, *c*, and *V*; Percentage of Thermal Coefficient (%TE); and Volume Instantaneous Thermal Expansion Coefficient (α_V) of Flux-Grown α-$GaPO_4$ at Various Temperatures

T (K)	ρ (g/cm^3)	*a* ()	%TE (*a*)	*c* ()	%TE (*c*)	*V* (^{3})	%TE (V)	α_V [10^{-5}/K]
303	3.5795	4.8968(2)	0	11.0332(3)	0	229.11(1)	0	2.874
373	3.5723	4.9012(2)	0.09	11.0360(3)	0.02	229.49(1)	0.17	2.891
473	3.5618	4.9069(2)	0.21	11.0400(4)	0.06	230.20(2)	0.47	2.995
673	3.5390	4.9210(2)	0.49	11.0503(4)	0.15	231.75(2)	1.15	3.492
873	3.5115	4.9365(2)	0.81	11.0641(4)	0.28	233.49(3)	1.91	4.367
973	3.4952	4.9461(3)	1.00	11.0721(4)	0.35	234.56(4)	2.38	4.940
1073	3.4769	4.9577(3)	1.25	11.0815(4)	0.44	235.88(4)	2.95	5.598
1123	3.4669	4.9631(3)	1.35	11.0858(5)	0.48	236.49(5)	3.22	5.961
1173	3.4562	4.9704(3)	1.50	11.0895(5)	0.51	237.26(5)	3.55	6.342

To study the thermal expansion properties of flux-grown α-$GaPO_4$, high-temperature powder X-ray diffraction (HTXRD) data were collected. A selection of HTXRD patterns recorded at various temperatures in the range of 303−1173 K is given in Figure 1. Their comparison shows that the overall XRD patterns remain the same from room temperature to 1173 K. A shift in position of Bragg reflections toward the lower angle side indicates an expansion in the lattice for the studied temperature domain.

The refined unit cell parameters for flux-grown $GaPO_4$ single crystals, with the low-quartz structure, at various temperatures, are presented in Table 2.

The variations of the lattice parameters and unit cell volumes with the temperature are shown in Figures 2 and 3.

Both the parameters and the volume increase markedly and nonlinearly as a function of the temperature. Their behavior with temperature *T* (in Kelvin) was fitted to a third-degree polynomial in the temperature increment ($T - 303$):

$$a(\text{Å}) = 4.896 + 6.366 \times 10^{-5}\,(T-303) - 1.342\times 10^{-8}\,(T-303)^2 + 4.290 \times 10^{-11}\,(T-303)^3 \quad (5)$$

$$c(\text{Å}) = 11.033 + 2.917 \times 10^{-5}\,(T-303) + 4.849\times 10^{-8}\,(T-303)^2 - 8.383 \times 10^{-12}\,(T-303)^3 \quad (6)$$

$$V(\text{Å}^3) = 229.115 + 6.586 \times 10^{-3}\,(T-303) - 5.293\times 10^{-8}\,(T-303)^2 + 3.766 \times 10^{-9}\,(T-303)^3 \quad (7)$$

The percentage of the mean linear thermal expansion (% TE) is given as[19]

$$\%\text{TE}(X) = 100\left\{\frac{(X_T - X_{303})}{X_{303}}\right\} \quad (8)$$

The calculated values of %TE(*a*), %TE(*c*), and %TE(*V*) are listed in Table 2. Both *a* and *c* lattice parameters expand as the temperature increases, but %TE(*a*) is 3-times larger than %TE(*c*). In the temperature range 303−1173 K, there is a strong anisotropy of the thermal expansion with a preferential expansion along the lattice parameter *a*. The *c*/*a* ratio decreases from 2.253 at 303 K to 2.231 at 1173 K. This may indicate a weaker Ga−O bond length within the *XY* planes than normal to the *XY* planes. These registered cell parameter evolutions with the temperature agree well with recent published results obtained from low-temperature hydrothermally grown $GaPO_4$ crystals using powder neutron diffraction.[20]

The lattice parameter expansions relative to room temperature were plotted as the temperature increment ($T - 303$). A fourth-degree polynomial expression of the corresponding graph gave the thermal expansion coefficients of the lattice parameters, in accordance with the Taylor series expansion:

$$\frac{\Delta X}{X(T_0)} = T^{(1)}_X \Delta T + T^{(2)}_X (\Delta T)^2 + T^{(3)}_X (\Delta T)^3 + T^{(4)}_X (\Delta T)^4 \quad (9)$$

where $\Delta T = T - T_0$ ($T_0 = 303$ K in this work) and with

$$T^{(n)}_X = \frac{1}{n! X(T)} \frac{\partial^n X}{\partial T^n}\Big|_{T=T_0} \quad (10)$$

The resulting thermal expansion coefficients relative to room-temperature are presented in Table 3 and are compared with published results[21,22] on hydrothermally grown α-$GaPO_4$ crystals.

We see that, concerning the first-order thermal expansion coefficients for both *a* and *c* lattice parameters, reasonable agreements are observed with previous reports, while concerning the higher-order coefficients, high inconsistencies are found. The discrepancies can be related to the different behavior with temperature existing between high-temperature flux-grown and low-temperature hydrothermally grown $GaPO_4$ materials, as already seen by thermal analyses.[23] The difference in the thermal behavior was explained by the negligible hydroxyl (OH) content measured in flux-grown crystals compared to those crystallized in acidic solutions at low-temperature (about 450 K).[6,21,22]

(19) Raju, S.; Sivasubramanian, K.; Divakar, R.; Panneerselvam, G.; Banerjee, A.; Mohandas, E.; Antony, M. P. *J. Nucl. Mater.* **2004**, *325*, 18.

(20) Haines, J.; Cambon, O.; Prudhomme, N.; Fraysses, G.; Keen, D. A.; Chapon, L. C.; Tucker, M. G. *Phys. Rev. B* **2006**, *73*, 014103.

(21) Krempl, P.; Krispel, F.; Wallnöfer, W.; Leuprecht, G. In *Proceedings of the 9th European Frequency and Time Forum*; ENSMM: Besançon, France, 1995; p 66.

(22) Reiter, C.; Krempl, P. W.; Tner, H.; Wallnöfer, W.; Worsch, P. M. *Ann. Chim. Sci. Mater.* **2001**, *26*, 91.

(23) Armand, P.; Beaurain, M.; Rufflé, B.; Menaert, B.; Balitsky, D.; Clement, S.; Papet, P. *J. Cryst. Growth* **2008**, *310*, 1455.

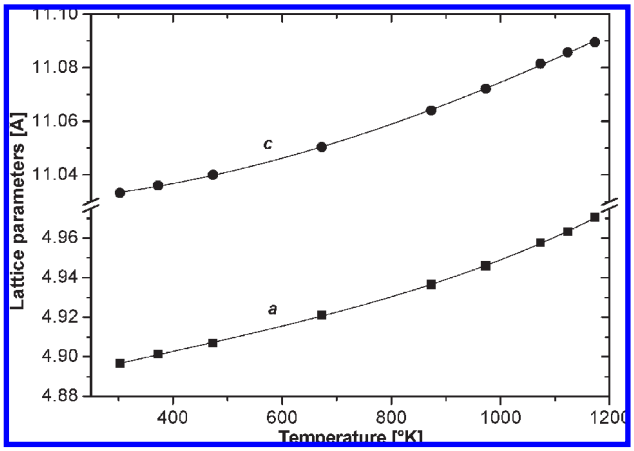

Figure 2. Lattice parameters of quartz-type $GaPO_4$ as a function of temperature. The solid line represents a third-order polynomial least-squares fit. The error bars are smaller than the symbol size.

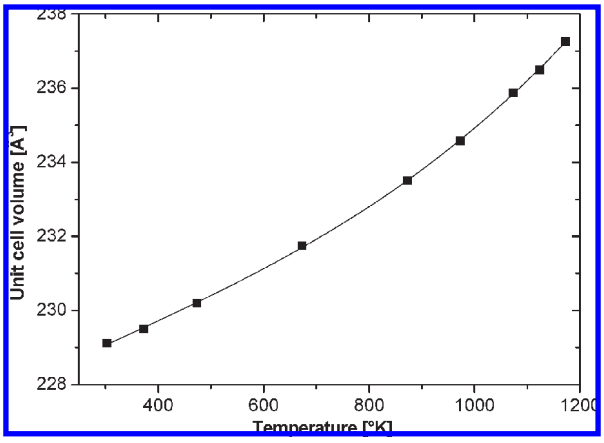

Figure 3. Unit cell volume of quartz-type $GaPO_4$ as a function of temperature. The solid line represents a third-order polynomial least-squares fit. The error bars are smaller than the symbol size.

Table 3. Thermal Expansion Coefficients of α-$GaPO_4$ Material

	flux-grown (this work)		hydrothermally grown[21]		hydrothermally grown[22]	
	a (x or *y* axis)	*c* (*z* axis)	*a* (x or *y* axis)	*c* (*z* axis)	*a* (x or *y* axis)	*c* (*z* axis)
$T^{(1)}$ [10^{-6} K^{-1}]	11.698	3.877	9.02	3.38	12.78	3.69
$T^{(2)}$ [10^{-9} K^{-2}]	5.012	−2.948	35.4	2.0	10.6	5.0
$T^{(3)}$ [10^{-12} K^{-3}]	−5.554	12.80	−99.1	1.0	−16.1	−5.4
$T^{(4)}$ [10^{-15} K^{-4}]	8.195	−7.76	98.8	4.5	12.3	3.6

To determine the volume instantaneous thermal expansion coefficients at constant pressure, we used the expression[24]

$$\alpha_V(T) = \frac{1}{V_T}\left(\frac{\partial V}{\partial T}\right)_P \quad (11)$$

The values are also listed in Table 2. The temperature dependence of the coefficients of the volume instantaneous linear thermal expansion yields the quadratic function:

$$\alpha_V(K^{-1}) = 3.291 \times 10^{-5} - 2.786 \times 10^{-8}[T] + 4.598 \times 10^{-11}[T]^2 \quad (12)$$

The calculated room temperature value $\alpha_V(303\ K) = 2.874 \times 10^{-5}\ K^{-1}$ is close to that of α-quartz-type $FePO_4$ ($2.924 \times 10^{-5}\ K^{-1}$)[25] and lower than those of hydrothermally grown α-quartz ($3.7 \times 10^{-5}\ K^{-1}$)[26] and berlinite ($3.97 \times 10^{-5}\ K^{-1}$).[27]

This room temperature expansion coefficient corresponds also to the first-order thermal coefficient[28] of unit cell volume, since

$$T^{(1)}_{C,V} = \frac{1}{V(303)}\frac{\partial V}{\partial T}|_{T=303} = \alpha_V(303\ K) \quad (13)$$

The room temperature experimental mass density of flux-grown α-$GaPO_4$ single crystals, determined by pycnometry using the helium displacement technique, is $\rho_0 = 3.5795 \pm 0.0005$ g/cm^3, which is almost consistent with the X-ray result ($\rho = 3.5801$ g/cm^3). We used the volume instantaneous thermal expansion function $\alpha_{V(T)}(K^{-1})$ given in eq 12 to calculate the density at each appropriate temperature, presented in Table 2, following the expression

$$\rho(T) = \rho_0 \exp(-\int_{303}^{T} \alpha_V(T)\, dT) \quad (14)$$

Acoustic-Mode Frequencies and Sound Velocities. Typical examples for the temperature dependence of the Brillouin spectrum obtained by the HRBS are shown in Figure 4. The dotted lines mark the position of two orders of the elastic line separated by the free spectral range of the spherical FP analyzer used here.

Figure 4a shows the softening with temperature of the γ_1 longitudinal acoustic mode related to C_{11}, whereas Figure 4b reveals a stiffening of the γ_2 transverse acoustic mode related to C_{66}. The frequency shift at which the γ_1 mode is observed depends on the polarization direction of the incident and scattered light as given by eq 2: 27.54 GHz at room temperature for polarizations along Z (n_o) and 27.23 GHz for polarizations along Y (n_e), in perfect agreement with the known birefringence of $GaPO_4$. Thanks to the high resolution of the experimental setup, we have been able to reveal the lifting of the degeneracy of the shear-wave velocities, a manifestation of the so-called *acoustical activity*, which is predicted to exist along the *c* axis in the uniaxial crystal class D_3.[29]

(24) Jackson, J. M.; Palko, J. W.; Andrault, D.; Sinogeikin, S. V.; Lakshtanov, D. L.; Wang, J.; Bass, J. D.; Zha, C. S. *Eur. J. Mineral.* **2003**, *15*, 469.
(25) Haines, J.; Cambon, O.; Hull, S. *Z. Kristallogr.* **2003**, *218*, 193.
(26) Ghiorso, M. S.; Carmichael, I. S. E.; Moret, L. K. *Contrib. Mineral. Petrol.* **1979**, *68*, 307.
(27) Maruoka, Y.; Kihara, K. *Phys. Chem. Miner.* **1997**, *24*, 243.
(28) Tarumi, R.; Nakamura, K.; Ogi, H.; Hirao, M. *J. Appl. Phys.* **2007**, *102*, 113508.
(29) Portugal, D. L.; Burstein, E. *Phys. Rev.* **1968**, *170*, 673.

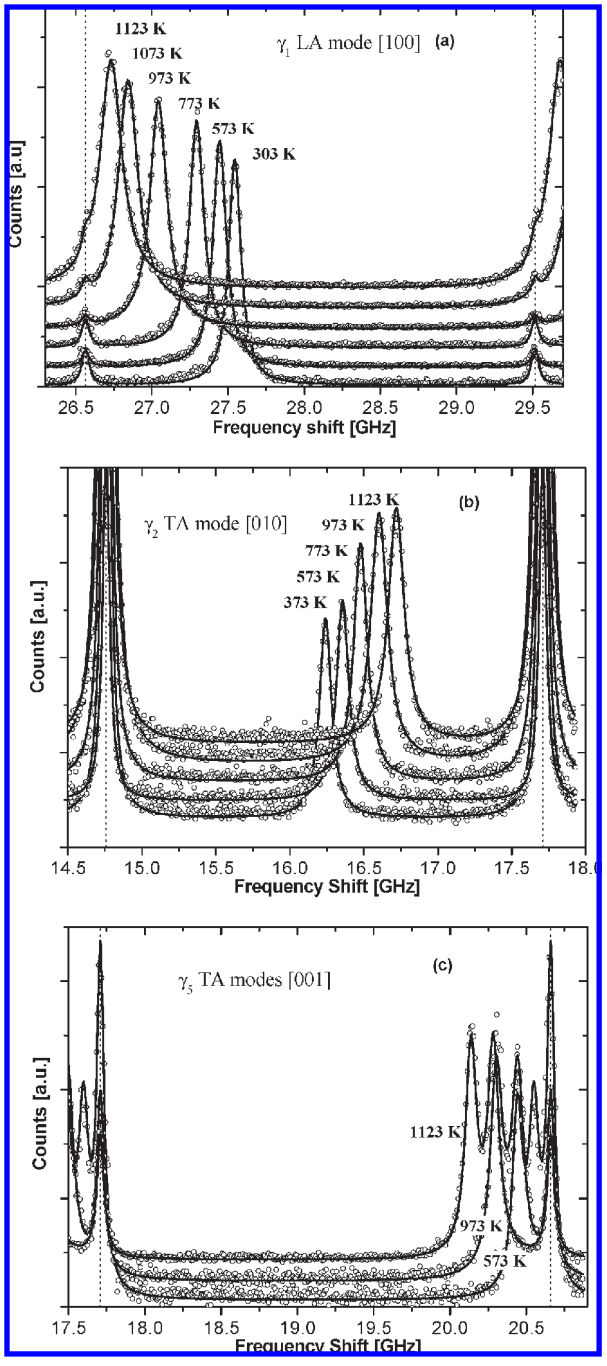

Figure 4. Brillouin spectra of a flux-grown $GaPO_4$ single crystal with the α-quartz structure: (a) γ_1 (C_{11}) longitudinal acoustic mode along X, (b) γ_2 (C_{66}) transverse acoustic mode along Y, and (c) shear-wave doublet γ_5 (C_{44}) along Z, obtained with linearly polarized laser light. The dotted lines mark the position of two orders of the elastic line separated by 2.95 GHz, the free spectral range of the SFP.

Figure 4c shows the temperature dependence of the shear-wave doublet γ_5, related to C_{44}. The Brillouin spectra have been obtained with linearly polarized laser light as the two transverse modes are right- and left-circularly polarized. At room temperature, the mean phonon frequency is $\Delta\nu_B$ = 20.454 GHz, whereas the doublet splitting is $\delta\Delta\nu_B$ = 94 MHz. The relative splitting is proportional to the wavevector or to the frequency $\delta v/\bar{v} = \gamma\Delta\nu_B$.[29] For $GaPO_4$, we found $\gamma = 2.2 \times 10^{-4}$ GHz^{-1}, a value slightly lower than the one found for α-SiO_2, $\gamma = 3.3 \times 10^{-4}$ GHz^{-1}.[30] Acoustical activity is the mechanical analogue of optical activity and is governed by the so-called acoustic gyrotropic tensor $d_{ij,1}$ related to the first-order spatial dispersion of the elastic constant C_{IJ}. For $GaPO_4$ we found $d_{54,3} = \gamma/(4\pi n_o)\delta v/\bar{v}$ = 4.4 N/m. As can be inferred from Figure 4c, $d_{54,3}$ increases significantly with the temperature, reaching 6.8 N/m at 1123 K.

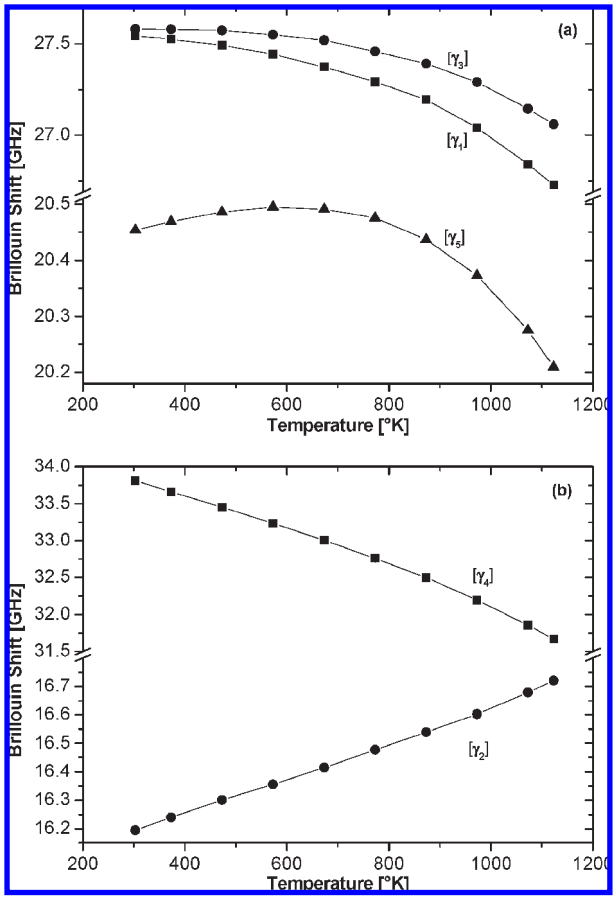

Figure 5. High-temperature Brillouin frequency shifts of a flux-grown $GaPO_4$ single crystal with the α-quartz structure. γ_1, γ_3, and γ_5 observed acoustic modes (as defined in Table 1) in part a, γ_2 and γ_4 acoustic modes in part b. The lines are guides for the eyes. The error bars are smaller than the symbol size.

The Brillouin shift, amplitude, and width of the modes were obtained by least-squares fits to the spectra. The standard errors given by the routine provide estimations of the Brillouin shift errors, which were below 0.01 GHz for all of the modes.

The temperature dependences of the Brillouin shifts for the five observed acoustic modes, plotted in Figure 5, were analyzed by means of the fourth-order Taylor series expansion as given by eqs 9 and 10.

The temperature coefficients of the Brillouin frequency shifts $T^{(n)}_{\nu B}$ relative to room-temperature, for X, Y, and Z simple orientations of α-quartz-structure $GaPO_4$ crystal, are summarized in Table 4.

With the use of eq 2, the sound velocities of the observed acoustic modes at different temperatures were calculated. The uncertainties in the velocities are estimated to be on the order of 1−3 m/s. The values of the room-temperature sound velocities compared with those obtained by Brillouin or pulse-echo methods on

(30) Pine, A. S. *Phys. Rev. B* **1970**, *2*, 2049.

Table 4. Room-Temperature Brillouin Shift $\nu_B(T_0)$ and Temperature Coefficients $T^{(n)}$ of the Measured Brillouin Frequency Shifts

modes	$\nu_B(T_0)$ [GHZ]	$T^{(1)}$ [10^{-6} K^{-1}]	$T^{(2)}$ [10^{-9} K^{-2}]	$T^{(3)}$ [10^{-12} K^{-3}]	$T^{(4)}$ [10^{-15} K^{-4}]
γ_1	27.543 ± 0.008	−6.31	−33.4	35.67	−48.02
γ_2	16.194 ± 0.015	40.20	−14.73	15.26	2.060
γ_3	27.581 ± 0.010	2.59	−28.95	25.04	−34.00
γ_4	33.813 ± 0.010	−62.17	−1.77	−5.07	−18.81
γ_5	20.454 ± 0.004	11.68	−13.39	−3.52	−23.33

Table 5. Comparison of Sound Velocities Registered for α-$GaPO_4$ Materials at Ambient Conditions

mode	V (m/s)[a] this work	V (m/s)[b] Brillouin[17]	V (m/s)[b] pulse-echo[6]	spread %
γ_1	4338 ± 2	4352	4337	0.35/0.02
γ_2	2565 ± 3	2539	2546	1.01/0.74
γ_3	4344 ± 2	4333	4358	0.25/0.32
γ_4	5387 ± 2	5348	5327	0.72/1.11
γ_5	3259 ± 1	3247	3254	0.37/0.15

[a] Flux-grown material. [b] Hydrothermally grown material.

hydrothermally grown samples, Table 5, are in good accordance for the whole three crystallographic faces selected to extract the elastic constants. The spread percentages never exceed the unit.

Single-Crystal Elastic Constants. Figure 6 presents the temperature dependence of the single-crystal elastic moduli C_{IJ} of flux-grown $GaPO_4$ from room temperature to 1123 K.

The constants C_{11}, C_{33}, C_{44}, and C_{12} show monotonic elastic softening upon heating, Figure 6a and b, while C_{66} and C_{14} show continuous stiffening, Figure 6c. Most of C_{IJ} change by only a few percent, while C_{14} increases by about 50% and C_{12} decreases by about 35%. The variations of C_{11}, C_{44}, C_{33}, and C_{66} look like those of the Brillouin frequency shift of the γ_1, γ_5, γ_4, and γ_2 modes (Figures 5 and 6).

Table 6 summarizes our values of the elastic constants C_{IJ} (GPa) calculated at room-temperature and compared with previous published data.[6,14,17,31] In all cases, C_{11} and C_{66} elastic constants were corrected for the piezoelectric effect, which had a value of 0.79×10^9 N m^{-2}. Since most of the previous set of data has used 3570 kg/m^3 as the room-temperature density value, we also calculated our elastic constants with this X-ray diffraction value for comparison, Table 6.

The elastic constant values given in ref 31 differ strongly from our data. This large divergence may be due to the small magnitude of the measured signal and poor quality of the hydrothermally grown samples used.[17] It is well-demonstrated that low-temperature hydrothermally grown α-$GaPO_4$ single crystals contain hydroxyl radicals, most often in high content for growth experiments done in the 80s, which enter the lattice during crystallization via the growth medium.[8,11] These OH groups, present as point defects, would reduce the lattice rigidity.

The set of data in ref 14, Table 6, was obtained from the measurement of the resonance frequencies of piezoelectrically excited vibrations of thin crystal plates of X and Y orientations. The α-$GaPO_4$ samples studied in ref 14 were also flux-grown under the same experimental conditions as those of the crystal used in this Brillouin study. The set of data in ref 14 presents a shear C_{66} value, which is 11% up from our C_{66} one, while the deduced C_{12} value is 36% less. Moreover, the reported longitudinal C_{11} value is only equal to 64.01 GPa in ref 14, while we found 66.52 GPa, Table 6 (or 66.4 GPa with ρ = 3570 kg/m^3).

The other published sets of elastic constants in refs 6 and 17 are in good agreement with our data with only 1−3% of divergence, except for the C_{14} elastic constant, for which a 30% divergence is noted, Table 6. For this C_{14}

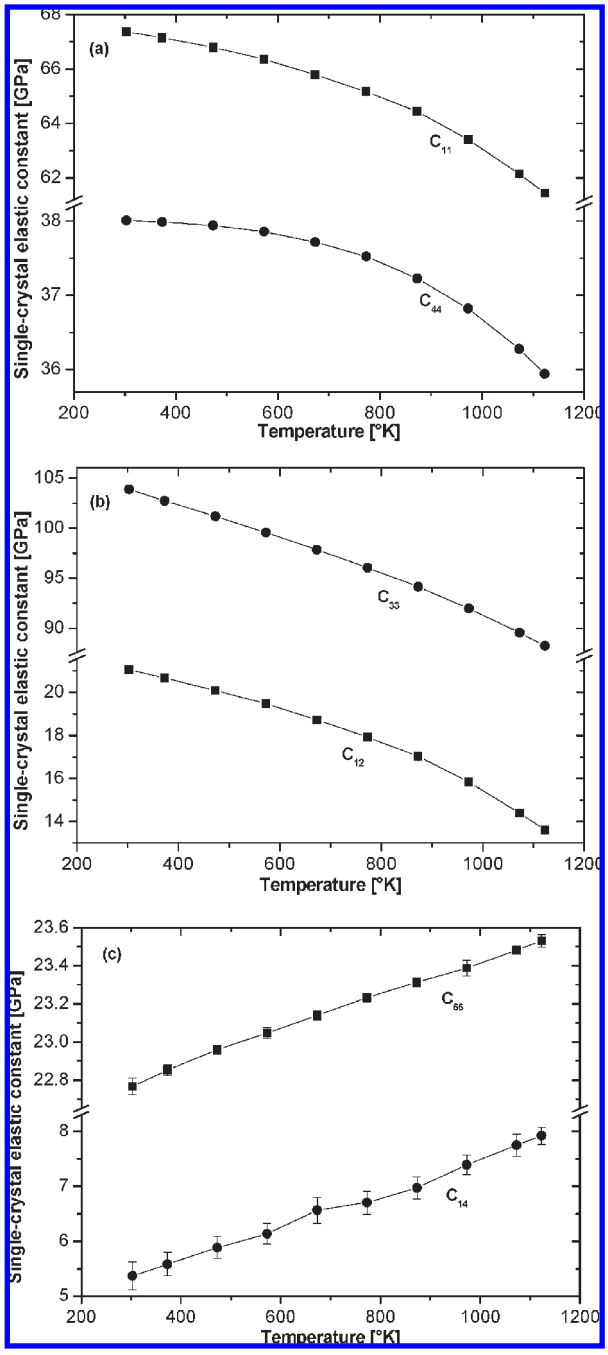

Figure 6. Temperature dependence of the elastic constants C_{IJ} of a flux-grown $GaPO_4$ single crystal with the α-quartz structure, C_{11} and C_{44} in part a, C_{33} and C_{12} in part b, and C_{66} and C_{14} in part c. The lines are guides for the eyes. The error bars are smaller than the symbol size.

(31) Engel, G.; Krempl, P.; Stadler, J. In *Proceedings of the 3rd European Frequency and Time Forum*; Gagnepain, J.-J., Ed.; ENSMM: Besançon, France, 1989; p 50.

Table 6. Comparison of Room-Temperature α-$GaPO_4$ Single-Crystal Elastic Constants at Constant Electric Field, Given in GPa

α-$GaPO_4$	C_{11}	C_{33}	C_{44}	C_{66}	C_{14}	$(C_{11} - 2C_{66}) = C_{12}$	ρ (kg/m^3)
hydro.-grown[31,a]	70.7	58.3	41.9	32.1	17.8	6.5	3570[d]
hydro.-grown[17,b]	66.58 ± 0.37	102.13 ± 0.55	37.66 ± 0.27	22.38 ± 0.32	3.91 ± 0.33	21.81 ± 1.01	3570[d]
hydro.-grown[6,c]	66.35 ± 0.02	101.31 ± 0.04	37.80 ± 0.01	22.35 ± 0.01	4.20 ± 0.308	21.65 ± 0.04	3570[d]
flux-grown[14,a]	64.01 ± 1.91		39.39 ± 1.17	25.25 ± 0.75	5.52 ± 0.717	13.51 ± 3.41	3571.4[d]
flux-grown (this work[b])	**66.52 ± 0.04**	**103.88 ± 0.06**	**38.01 ± 0.01**	**22.74 ± 0.04**	**5.53 ± 0.25**	**21.04 ± 0.12**	**3579.5[e]**
Flux-grown (this work[b])	*66.40*	*103.60*	*37.91*	*22.70*	*5.52*	*21.00*	*3570[d]*

[a] Resonance frequencies of plate. [b] Brillouin spectroscopy. [c] Pulse-echo method. [d] Mass density based on X-ray diffraction lattice parameters. [e] Our experimental mass density.

Table 7. Temperature Coefficients $T^{(n)}$ of the Single-Crystal Elastic Moduli of Flux-Grown α-$GaPO_4$

elastic moduli [GPa]	$T^{(1)}$ [10^{-6} K^{-1}]	$T^{(2)}$ [10^{-9} K^{-2}]	$T^{(3)}$ [10^{-12} K^{-3}]	$T^{(4)}$ [10^{-15} K^{-4}]
C_{11}	−42.41	−61.47	43.97	−82.46
C_{33}	−153.5	8.718	−37.33	−21.81
C_{44}	−5.863	−22.52	−33.53	−35.36
C_{66}	53.29	−29.32	12.71	5.460
C_{14}	586.0	−27.09	−338.1	452.1
C_{12}	−249.4	−131.0	111.6	−272.6

single-crystal elastic modulus, our calculated value is, on the contrary, in perfect agreement with the one obtained in ref 14 using the resonance frequency method on the same types of samples. Thus, using two different methods and two different samples, the same 5.52 GPa value was found for the C_{14} single-crystal elastic constant of flux-grown α-$GaPO_4$. Except for the C_{11} constant, the value of which being very comparable to those measured on hydrothermally grown $GaPO_4$ materials,[6,17] the C_{33}, C_{44}, C_{66}, and C_{14} elastic constant values are slightly higher for our material, and consequently the deduced C_{12} value is slightly smaller, Table 6.

The temperature dependences of the single-crystal elastic moduli, Figure 6, were analyzed by means of the fourth-order Taylor series expansion as given by eqs 9 and 10. The temperature coefficients $T^{(n)}$ ($n = 1-4$) obtained for each single-crystal elastic constant are presented in Table 7 for the flux-grown material.

The first-order temperature coefficients $T_{C_{IJ}}{}^{(1)}$ are negative for C_{11}, C_{33}, C_{44}, and C_{12} elastic constants, in perfect agreement with previous reports[6,14,22,31−33] on low-temperature hydrothermally grown α-$GaPO_4$ crystals. Our whole set of first-order temperature coefficients $T_{C_{IJ}}{}^{(1)}$ is in good accordance with previous reports presented in Table 8 and especially with results from refs 22 and 32.

We can notice that, except for $T_{C_{11}}{}^{(1)}$, for which our value is the lowest compared with the one in refs 22 and 32, Table 8, our first-order temperature coefficients of the single-crystal elastic constants are always higher than those reported in refs 22 and 32.

It is important to recall that it is the same as-grown sample shaped as a cube with X, Y, and Z faces which was used for the whole set of Brillouin measurements from room to high temperatures. This high-temperature flux-grown α-$GaPO_4$ sample was heated several times up to 1123 K without presenting the well-known

Table 8. First-Order Temperature Coefficient of the Single-Crystal Elastic Constants C_{IJ} Obtained for α-$GaPO_4$ Material

α-$GaPO_4$ growth method	T_{C11} [10^{-6} K^{-1}]	T_{C33} [10^{-6} K^{-1}]	T_{C44} [10^{-6} K^{-1}]	T_{C66} [10^{-6} K^{-1}]	T_{C12} [10^{-6} K^{-1}]	T_{C14} [10^{-6} K^{-1}]
hydrothermal[31]	−37	−118		31		
hydrothermal[8,a]	−51.2	−123	−4.4	47.2	−242	520
hydrothermal[6]	−65	−103.0	−14.1	28.1	−257.2	200.4
hydrothermal[33]	−63	−135	−62	69	−335	825
hydrothermal[22,b]	−44.1	−127.5	−0.4	44.9	−226.7	507.2
flux[c]	−42.41	−153.5	−5.863	53.29	−249.4	586.0

[a] Studied temperature range: 100−700 K. [b] Studied temperature range: 223−973 K. [c] Studied temperature range: 303−1123 K.

"milky" hue (opaque) which reduces the quality of the crystals obtained by the low-temperature hydrothermal method.[32] This effect has been attributed to the release with temperature of water from hydroxyl impurities.

As already shown by infrared spectroscopy,[4,23] our flux-grown $GaPO_4$ sample can be considered as an OH-group-"free" crystal, which could explain why it was not affected by successive thermal cycles from 303 to 1123 K. Furthermore, the thermal behavior of these samples differs from that of hydrothermally grown materials since we have registered for the flux-grown $GaPO_4$ crystals a totally reversible α-quartz ↔ β-cristobalite transition. This behavior could be directly related to the negligible OH content in flux-grown $GaPO_4$ single crystals.

The change in the values of the elastic constants with the growth technique is generally associated with some modifications of the lattice by intrinsic point defects, impurities, dislocations, and so forth. It is well-known that the propagation velocity into a medium is governed by the atomic bond strength and that each structural defect produces some distortions of the lattice which may, locally, modify its rigidity. The strong reduction of the OH concentration in the lattice of high-temperature flux-grown α-$GaPO_4$ is believed to have induced an improvement of the lattice rigidity. This would be the main effect acting for the slightly higher values of most of the elastic constants measured on flux-grown $GaPO_4$ material, Table 6.

The results obtained from infrared studies (OH content), thermal behavior analysis, and Brillouin scattering experiments on our flux-grown $GaPO_4$ single crystals are very encouraging. They show that the flux technique could be a growth method to produce piezoelectric crystals with very promising application potential.

Therefore, the difficulty consists now in getting larger α-$GaPO_4$ single crystals of appropriate size and habit for further technical applications. In this context, the use of seeds with the top seeding solution growth technique could be very interesting to develop.

(32) Wallnöfer, W.; Stadler, J.; Krempl, P. In *Proceedings of the 7th European Frequency and Time Forum*; ENSMM: Besançon, France, 1993; p 653.

(33) Krempl, P.; Schleinzer, G.; Wallnöfer, W. *Sens. Actuators* **1997**, *A61*, 361.

Conclusion

We were able to produce OH-free single crystals of the piezoelectric phase of $GaPO_4$ using the high-temperature flux-grown technique. Brillouin scattering experiments made at room and high temperatures were undertaken on a crystal shaped as a cube with X, Y, and Z faces. The sample was heated several times up to 1123 K without presenting the well-known "milky" hue. The room-temperature single-crystal elastic constants C_{IJ} of our flux-grown sample are in very good agreement with most of the published sets of data concerning hydrothermally grown α-$GaPO_4$ materials. Therefore, the C_{IJ} of the flux-grown sample presents slightly higher values, especially for the C_{33} and C_{14} constants. Again, the first-order temperature coefficients of the elastic constants relative to room temperature are in the same range of order as the published ones and present a particularly good agreement with the latest report on hydrothermally grown $GaPO_4$ single crystals.

Compared with low-temperature hydrothermally grown $GaPO_4$ crystals, the strong reduction of the OH concentration in the lattice of high-temperature flux-grown α-$GaPO_4$ is believed to have induced an improvement of the lattice rigidity. This would be the main effect acting for the slightly higher values of most of the elastic constants measured on flux-grown $GaPO_4$ samples.

This result coupled with a remarkable thermal behavior made these flux-grown α-$GaPO_4$ single crystals very promising materials as compared with α-$GaPO_4$ grown using low-temperature methods. However, the production for technical applications of flux-grown α-$GaPO_4$ single crystals with both a sufficient size and a low level of structural defects needs further investigation.

Acknowledgment. The authors thank Dr. Bernard Fraisse (ICGM, AIME team, Montpellier, France) for powder X-ray diffraction data collection from room to high temperatures.